J Physiol 589.7 (2011) pp 1571–1585

The Journal of Physiology

Desensitization of neurotransmitter-gated ion channels during high-frequency stimulation: a comparative study of Cys-loop, AMPA and purinergic receptors

David Papke[1], Giovanni Gonzalez-Gutierrez[1,2,3] and Claudio Grosman[1,2,3]

[1]*Neuroscience Program,* [2]*Department of Molecular and Integrative Physiology and* [3]*Center for Biophysics and Computational Biology, University of Illinois at Urbana-Champaign, Urbana, IL 61801, USA*

Non-technical summary During fast synaptic transmission, series of brief pulses of highly concentrated neurotransmitter impinge repetitively on the postsynaptic membrane. The number of neurotransmitter-gated ion channels (NGICs) that open in response to each neurotransmitter pulse may increase or decrease along such trains of stimuli to an extent that can affect the transmission of action potentials. This 'short-term' plasticity results from transient changes (lasting from milliseconds to minutes) in the properties of the presynaptic terminal, the postsynaptic terminal, or both. In this paper, we studied eight representative members of all three known superfamilies of NGICs to determine the extent to which short-term plasticity can occur at the postsynaptic-receptor level. We found that the responsiveness of all tested channels declines appreciably along trains of brief neurotransmitter pulses delivered at physiologically relevant frequencies. We suggest that the role of receptor desensitization in the synaptic control of action-potential transmission may be more general than previously thought.

Abstract Changes in synaptic strength allow synapses to regulate the flow of information in the neural circuits in which they operate. In particular, changes lasting from milliseconds to minutes ('short-term changes') underlie a variety of computational operations and, ultimately, behaviours. Most studies thus far have attributed the short-term type of plasticity to activity-dependent changes in the dynamics of neurotransmitter release (a presynaptic mechanism) while largely dismissing the role of the loss of responsiveness of postsynaptic receptor channels to neurotransmitter owing to entry into desensitization. To better define the response of the different neurotransmitter-gated ion channels (NGICs) to repetitive stimulation without interference from presynaptic variables, we studied eight representative members of all three known superfamilies of NGICs in fast-perfused outside-out patches of membrane. We found that the responsiveness of all tested channels (two nicotinic acetylcholine receptors, two glycine receptors, one GABA receptor, two AMPA-type glutamate receptors and one purinergic receptor) declines along trains of brief neurotransmitter pulses delivered at physiologically relevant frequencies to an extent that suggests that the role of desensitization in the synaptic control of action-potential transmission may be more general than previously thought. Furthermore, our results indicate that a sizable fraction (and, for some NGICs, most) of this desensitization occurs during the neurotransmitter-free interpulse intervals. Clearly, an incomplete clearance of neurotransmitter from the synaptic cleft between vesicle-fusion events need not be invoked to account for NGIC desensitization upon repetitive stimulation.

(Received 30 November 2010; accepted after revision 2 February 2011; first published online 7 February 2011)
Corresponding author C. Grosman: University of Illinois at Urbana-Champaign, 407 S. Goodwin Ave. 524 Burrill Hall, Urbana, IL 61801, USA. Email: grosman@illinois.edu

Abbreviations GlyR, glycine receptor; NGIC, neurotransmitter-gated ion channel; $P2X_2R$, purinergic ionotropic type 2 receptor.

DOI: 10.1113/jphysiol.2010.203315

Introduction

During fast synaptic transmission, series of brief pulses (<1 ms in duration; Magleby & Stevens, 1972; Clements, 1996; Dudel *et al.* 1999) of highly concentrated neurotransmitter impinge on the postsynaptic membrane at frequencies at least as high as ∼200 Hz (Hennig & Lømo, 1985; Saviane & Silver, 2006). The peak postsynaptic response to each pulse may increase or decrease along such trains to an extent that can affect the transmission of action potentials. In turn, this phenomenon allows synapses to perform a variety of computational tasks underlying behaviours as diverse as sound localization, sensory adaptation, the processing of moving sensory images and intestinal peristalsis (Fortune & Rose, 2001; Stevens, 2003; Abbott & Regehr, 2004; Grande & Spain, 2005). This 'short-term' plasticity results from transient changes (lasting from milliseconds to minutes) in some of the properties of the presynaptic terminal, the postsynaptic terminal, or both (Zucker & Regehr, 2002).

Most studies thus far have attributed the origin of short-term synaptic plasticity to presynaptic changes, including changes in the probability of synaptic-vesicle fusion and the size of the pool of release-ready vesicles (Zucker & Regehr, 2002). Moreover, even changes in the number of neurotransmitter molecules per vesicle and variations in the kinetics and extent of fusion-pore opening have been suggested to play a role (Chen *et al.* 2004). The involvement of postsynaptic changes, on the other hand (specifically, the progressive loss of ionotropic-receptor responsiveness to neurotransmitter owing to desensitization), has received much less attention and has been dismissed for most synapses with the exception of some glutamatergic synapses involved in the processing of motor (Wall *et al.* 2002), visual (Chen *et al.* 2002) and auditory information (Otis *et al.* 1996; Brenowitz & Trussell, 2001; Wong *et al.* 2003; Koike-Tani *et al.* 2008; Chanda & Xu-Friedman, 2010). We surmise that the little consideration given so far to postsynaptic mechanisms stems, at least to some extent, from the common misconception that desensitization can only take place while neurotransmitter is present in the extracellular solution. This idea is often followed by the inference that, since neurotransmitter is present in the synaptic cleft for only very brief intervals at a time and since entry into desensitization is comparatively slow, the extent of desensitization during synaptic transmission must be negligible.

Desensitization during long stretches of repetitive stimulation has been demonstrated to occur for some neurotransmitter-gated ion channels (NGICs) (Raman & Trussell, 1995; Paradiso & Brehm, 1998; Pugh & Raman, 2005), but it is unknown whether this phenomenon is a general property of all wild-type members of this class of postsynaptic membrane receptor. Such a finding would suggest a novel functional role for the well-conserved desensitized state(s), an often-overlooked aspect of postsynaptic-channel function, during information processing in the nervous system (Jones & Westbrook, 1995, 1996).

Unfortunately, disentangling the relative contributions of presynaptic and postsynaptic events to short-term plasticity using intact synapse preparations is not trivial because measurement of the postsynaptic response to presynaptic stimulation necessarily depends on both facets of transmission. And although methods to selectively block the presynaptic or postsynaptic contributions have been developed for some neurotransmitters (such as the use of cyclothiazide or concanavalin A to slow down the desensitization of glutamate receptor channels; Partin *et al.* 1993; Yamada & Tang, 1993), the reports produced thus far remain somewhat conflicting.

We decided to isolate the postsynaptic contribution to short-term depression in a manner that minimizes the ambiguities associated with the study of intact synapses. To this end, we studied the responses of representative members of all three known superfamilies of NGICs to the repetitive application of brief pulses of neurotransmitter in fast-perfused outside-out patches of membrane. Our results indicate that the peak-current responses of all tested NGICs decrease appreciably along trains of high-frequency stimulation. This observation suggests (a) that desensitization of postsynaptic receptor channels may well be a general mechanism contributing to short-term synaptic depression, and (b) that synapses that support reliable synaptic transmission must bear specific adaptations that reduce the impact of the progressive loss of responsiveness to neurotransmitter.

Methods

cDNA clones, mutagenesis and heterologous expression

Complementary DNA (cDNA) clones encoding the adult mouse muscle AChR subunits (accession numbers: α1, P04756; β1, P09690; δ, P02716; ε, P20782) were provided by S. M. Sine (Mayo Clinic College of Medicine, Rochester, MN, USA); cDNAs for the rat GluA1-flip (accession number: P19490-2) and rat GluA2-flop (RNA-edited form, that is, containing the Q608R and R743G variants; accession number: P19491-1) AMPAR subunits by I. Greger (MRC Laboratory of Molecular Biology, Cambridge, UK); cDNAs for the rat $GABA_AR$ α1, β1 and γ2L subunits (accession numbers: α1, P62813; β1, P15431; γ2L, Q6PW52) by J. Fisher (University of South Carolina School of Medicine, Columbia, SC, USA); cDNA for the rat purinergic ionotropic type 2 receptor ($P2X_2R$) (accession number: P49653) by A.

Surprenant (University of Manchester, Manchester, UK); cDNA for the rat glycine receptor (GlyR) α1 subunit isoform b (accession number: P07727-2) by M. M. Slaughter (University at Buffalo, Buffalo, NY, USA); and cDNA for the human GlyR β subunit (accession number: P48167) by P. R. Schofield (School of Medical Sciences, University of New South Wales, Sydney, NSW, Australia). To convert the rat GlyR α1 subunit open reading frame into its human counterpart (accession number: P23415) we engineered the required mutations (F9L, D27E, D354E, G357A, N388S, A394P and K449Q) using a QuikChange site-directed mutagenesis kit (Stratagene). cDNAs for the human AChR α3, α5 and β4 subunits were purchased from Open Biosystems (accession numbers: α3, P32297; α5: P30532-1; β4, P30926) and were subcloned into pcDNA3.1. These neuronal-AChR subunit cDNAs were cotransfected with cDNA encoding human RIC-3 isoform 1 (accession number: Q7Z5B4-1, provided by W. N. Green, University of Chicago, Chicago, IL, USA) a chaperone that appeared to enhance the expression of these AChRs in our experiments (as judged from the larger peak amplitudes of the recorded currents) in keeping with previous reports (Lansdell *et al.* 2005). Human embryonic kidney (HEK)-293 cells were transiently transfected with cDNA using a calcium phosphate precipitation method.

Electrophysiology

Agonist-concentration jumps were applied to outside-out patches using a two-barrelled glass-capillary 'θ-tube' (Hilgenberg, Malsfeld, Germany) through which two solutions flow, as described by Jonas (1995; see also Elenes *et al.* 2006, 2009). The θ-tube was mounted on a piezo-electric device (Burleigh-LSS-3100; Lumen Dynamics Group Inc., Mississauga, Canada), the movement of which was controlled using a Digidata 1322A interface and pCLAMP 9.0 software (both from Molecular Devices, Sunnyvale, CA, USA). To ensure smooth θ-tube movements, the computer-generated signals to the piezo-electric device were low-pass filtered (900C, Frequency Devices, Ottawa, IL, USA) at a cutoff frequency between 125 and 150 Hz. The time course of solution exchange achieved with this system ($t_{10-90\%} = 102\,\mu$s; $t_{90-10\%} = 110\,\mu$s) was estimated by measuring the liquid-junction potential developed when alternately exposing the tip of an open patch pipette to a 1 M KCl solution (for ~1 ms) and a 140 mM KCl solution (for ~20 ms) flowing through the two barrels of the θ-tube, as described previously (Elenes *et al.* 2006). Ensemble ('macroscopic') currents were recorded at −80 mV (unless otherwise indicated) and room temperature using an Axopatch 200B amplifier (Molecular Devices) and were digitized at 100 kHz; the effective bandwidth before analysis was DC–10 kHz. Single-channel current–voltage (I–V) data were recorded in the cell-attached configuration at room temperature using an Axopatch 200B amplifier (Molecular Devices) and were digitized at 100 kHz; the effective bandwidth before analysis was DC–20 kHz.

Solutions

For macroscopic-current recordings, outside-out patches were alternately exposed to two solutions differing only in the presence or absence of agonist. Apart from the agonist concentration, this solution consisted of (in mM): 142 KCl, 5.4 NaCl, 1.8 $CaCl_2$, 1.7 $MgCl_2$, 10 Hepes/KOH, pH 7.4. The pipette solution consisted of (in mM): 100 KF, 40 KCl, 1 $CaCl_2$, 11 EGTA, and 10 Hepes/KOH, pH 7.4. As in our previous work (Elenes *et al.* 2006, 2009), the presence of fluoride in the pipette solution appeared to increase the stability of fast-perfused outside-out patches. For cell-attached, single-channel recordings, we used the same solution in the patch pipette as in the bath, the only difference being the presence of agonist in the pipette. The composition of this solution was (in mM): 142 KCl, 5.4 NaCl, 1.8 $CaCl_2$, 1.7 $MgCl_2$, 10 Hepes/KOH, pH 7.4. For every receptor, the natural neurotransmitter was used as the agonist; their concentrations were: 1 mM ACh, 1–10 mM GABA, 1–10 mM Gly, 10 mM Glu and 0.85 mM ATP.

Pulse protocols and data analysis

Macroscopic data were analysed using pCLAMP 9.0 (Molecular Devices) and SigmaPlot 7.101 (Systat Software Inc., San Jose, CA, USA), whereas single-channel data were idealized using the SKM option in QuB software (Qin, 2004) (www.qub.buffalo.edu). To characterize the time course of deactivation, we applied short (1 ms) pulses of neurotransmitter at saturating concentrations in the form of low-frequency trains (for the $P2X_2R$, we applied trains of 10 pulses at 0.125 Hz or trains of 25 pulses at 1 Hz; for all other NGICs studied here, we applied trains of 25 pulses at 1 Hz). The responses to individual pulses were averaged within each train (one train per patch), and these averaged traces were fitted with an exponential function from the peak of the transient through the end of any observable current. The resulting time constants were averaged across patches and are listed in Table 1. To characterize the time course of entry into desensitization, we applied long (2–5 s) applications of neurotransmitter at saturating concentrations. The resulting current traces were fitted with an exponential function from the peak of the transient through either the end of the agonist pulse or the end of any observable current (whichever came first). The resulting time constants were averaged across patches and are listed in Table 1. To characterize

Table 1. Kinetic parameters of channel deactivation and desensitization

NGIC	$\tau_{deactivation}$ (ms)[a]	$\tau_{entry\ into\ desensitization}$ (ms)[a]	$\tau_{recovery}$ (ms)
$\alpha1\beta1\delta\varepsilon$ AChR	1.11 ± 0.05	45.7 ± 9.94 (0.70 ± 0.08)	267 ± 11
		516 ± 172 (0.30 ± 0.08)	
$\alpha1\beta1\gamma$2L $GABA_AR$	2.94 ± 0.64 (0.67 ± 0.04)	2.56 ± 0.39 (0.60 ± 0.03)	3, 650 ± 170
	22.5 ± 8.26 (0.33 ± 0.04)	86 ± 26 (0.15 ± 0.03)	
		2, 569 ± 496 (0.25 ± 0.03)	
$\alpha1$ GlyR	3.97 ± 0.77 (0.67 ± 0.06)	3.76 ± 1.37 (0.49 ± 0.07)	476 ± 153 (0.39 ± 0.07)
	23.1 ± 4.8 (0.33 ± 0.06)	77.5 ± 17.6 (0.22 ± 0.05)	6, 210 ± 880 (0.61 ± 0.07)
		1, 316 ± 400 (0.29 ± 0.04)	
$\alpha1\beta$ GlyR	4.90 ± 0.63 (0.61 ± 0.05)	5.54 ± 0.88 (0.24 ± 0.05)	866 ± 277 (0.46 ± 0.11)
	29.0 ± 3.5 (0.39 ± 0.05)	107 ± 16 (0.19 ± 0.04)	6, 420 ± 1, 300 (0.54 ± 0.11)
		3, 833 ± 796 (0.58 ± 0.05)	
GluA1 AMPAR	0.57 ± 0.04	2.65 ± 0.17	214 ± 12
GluA1/2 AMPAR	0.57 ± 0.07	2.10 ± 0.16	120 ± 11
$P2X_2R$	23.3 ± 2.6 (0.43 ± 0.05)	47.7 ± 6.1 (0.37 ± 0.04)	18, 100 ± 1, 380
	85.8 ± 11.9 (0.57 ± 0.05)	378 ± 71 (0.63 ± 0.04)	

[a]Mean (± standard error) values of time constants estimated as indicated in Methods. Where applicable, normalized amplitudes are shown in parentheses. All shown estimates correspond to recordings obtained from outside-out patches within 2 and 5 min upon attaining the whole-cell configuration ('early time' in Supplemental Table 2). Considerable patch-to-patch variability was observed for the kinetics of deactivation and, especially, entry into desensitization at the level of both time constant/amplitude values and number of exponential components (see Supplemental Table 1). For each receptor, the mean values in this table correspond to those calculated by averaging the time constant and amplitude estimates obtained only from the subset of traces that were best fitted with the most common number of components.

the time course of recovery from desensitization, we applied pairs of conditioning (1 s) and test (100 ms) pulses of neurotransmitter at saturating concentrations with agonist-free interpulse intervals of variable duration. The interval between any two consecutive pairs of pulses was adjusted for each receptor so as to ensure complete recovery from desensitization before application of each new conditioning pulse. The fraction of receptor channels that recovered at the end of each interpulse interval was calculated as the peak response to the test pulse minus the current at the end of the corresponding conditioning pulse divided by the difference between the peak response to the conditioning pulse and the current at the end of it. Plots of the fraction of recovered receptors as a function of the duration of the interpulse intervals were well fitted with either mono- or double- exponential-rise functions. The corresponding time constants are listed in Table 1. To characterize the response to repetitive stimulation, we applied trains of 1 ms pulses of saturating neurotransmitter at variable frequencies. High patch-to-patch variability complicated our analysis of macroscopic recordings. Quite notably, the number of exponential components that was deemed necessary to fit the macroscopic responses varied from patch to patch for any given receptor (Supplemental Table 1).

Expression of heteromeric glycine and AMPA receptors

Both homomeric ($\alpha1$) and heteromeric ($\alpha1\beta$) GlyRs can form. To favour the expression of the heteromeric receptor, we transfected subunit cDNAs at a 40:1 β:$\alpha1$ ratio, as suggested by Sivilotti and coworkers (Burzomato *et al.* 2004). Under these conditions, we observed only one burst of single-channel openings with a conductance corresponding to that of the $\alpha1$-subunit homomer (105 ± 2 pS; all other bursts had a conductance of 54 ± 1 pS) out of >500 total bursts recorded in 10 cell-attached patches obtained from different cells. As is the case for the GlyRs, both homomeric (GluA1) and heteromeric (GluA1/2) AMPARs can form. Additionally, GluA2 homomers can also form, but the extremely low single-channel conductance of the Q/R RNA-edited form of these channels (the one we used here) prevents them from making an appreciable contribution to the macroscopic currents (Swanson *et al.* 1997). To favour the expression of the heteromeric receptor, we transfected subunit cDNAs at a 10:1 GluA2:GluA1 ratio. To assess the validity of this approach, we generated macroscopic *I–V* relationships in the presence or absence of spermine (a pore blocker of the homomeric, but not the heteromeric, channel; Kamboj *et al.* 1995), in the pipette of outside-out

patches. Supplemental Fig. 1 shows the block by spermine of, mostly, the outward currents through homomeric GluA1 receptors and the absence of blocking effect on the population of receptors expressed upon transfection with the 10:1 GluA2:GluA1 cDNA mixture. We conclude that this ratio of cDNAs leads to the expression of mostly heteromeric GluA1/2 receptors in the membrane of HEK-293 cells.

Results

All known NGICs (including even their bacterial homologues; Gonzalez-Gutierrez & Grosman, 2010) can desensitize, that is, enter a set of non-conductive conformations that, when fully bound to ligand, become the most stable states of the channel (e.g. Katz & Thesleff, 1957; Magleby & Pallotta, 1981; Liu & Dilger, 1992; Franke *et al.* 1993; Paradiso & Brehm, 1998; Robert & Howe, 2003). Thus, when exposed to saturating concentrations of neurotransmitter (as may be the case for those channels directly aligned with release-ready vesicles right after a vesicle-fusion event), NGICs interconvert several times between fully liganded closed- and open-channel conformations until, eventually, they desensitize. Of course, the neurotransmitter can dissociate from the channel during this period, but re-binding is so fast under saturating conditions that unbinding can be safely ignored. On the other hand, when the concentration of neurotransmitter drops to zero (as may be the case between vesicle-fusion events), the fully liganded NGICs that have not already desensitized keep interconverting among closed and open conformations but now, since re-binding is extremely unlikely, bursts of closed-open channel interconversions can also be terminated by neurotransmitter dissociation. It follows, then, that NGICs exposed to 'synaptic-like', repetitive applications of neurotransmitter can desensitize not only within, but also between, pulses even if the clearance of neurotransmitter between pulses were complete and infinitely fast. Within neurotransmitter pulses, the extent of desensitization is limited by the comparatively short lifetime of neurotransmitter in the synaptic cleft whereas, during the much longer interpulse intervals, entry into desensitization is limited by the fact that neurotransmitter dissociation provides an alternative route for channel deactivation. Despite these limitations, however, the fraction of channels that enter desensitized states upon repetitive stimulation need not be negligible. Furthermore, because recovery from desensitization takes time, repeated exposure to neurotransmitter may lead to the progressive decline of the peak-current amplitudes.

The extent to which the peak currents decrease upon repetitive stimulation depends on the particular values of the rate constants governing the behaviour of each channel, on the concentration of neurotransmitter, and on the frequency of the stimulus train. As a result, this decline could range from negligible to a situation in which only the first pulse in a train elicits a measurable current transient. Because the response of an NGIC to a train of stimuli cannot be easily inferred from the channel's response to other types of ligand applications, we set out to determine the extent of this decline experimentally.

NGICs desensitize appreciably during deactivation

Figure 1 shows representative responses of members of all three superfamilies of NGICs (namely, the Cys-loop,

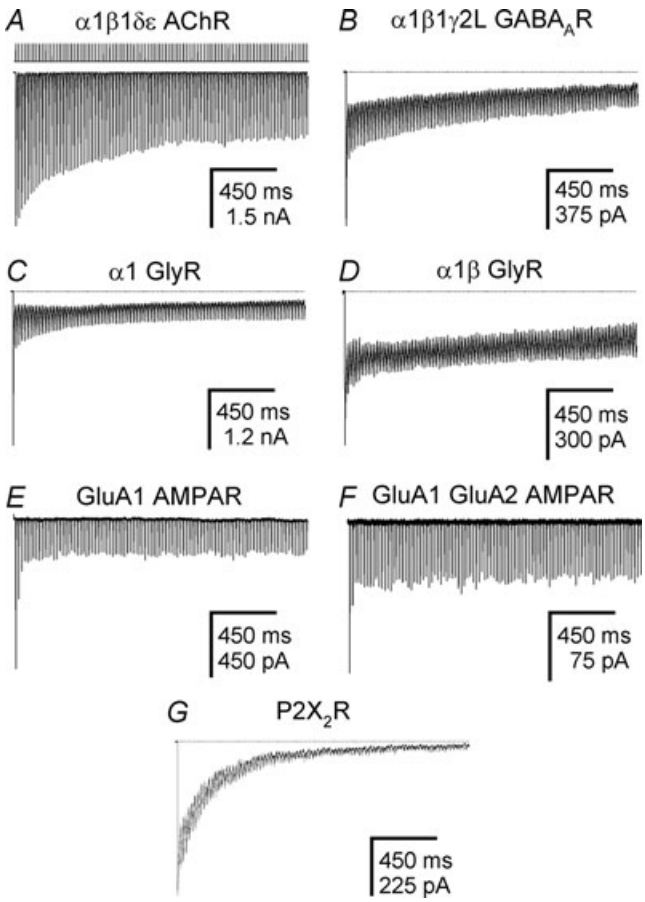

Figure 1. Peak-current depression upon repetitive stimulation
A–G, current traces recorded from individual outside-out patches. Each panel is the response of a different NGIC to the application of a 50 Hz train of 1 ms pulses of saturating neurotransmitter. One such train is indicated in *A* above the current trace. The zero-current level is indicated with a dotted line. The concentration of neurotransmitter was 1 mM ACh, 10 mM GABA, 10 mM Gly, 10 mM Glu and 0.85 mM ATP for the AChR, the GABA$_A$R, the GlyRs, the AMPARs and the P2XR, respectively. Although the responses recorded from individual patches exhibited high patch-to-patch variability, the traces shown are representative of the average behaviour of each receptor. The larger extent of desensitization observed for the muscle AChR compared to that reported earlier (Elenes *et al.* 2006, 2009) is very likely to be due to the use of a higher concentration of ACh in the experiments reported here (1 mM instead of 100 μM).

excitatory-glutamate and purinergic receptor channels) to trains of 1 ms pulses of saturating neurotransmitter applied at 50 Hz, a physiologically relevant frequency. These channels are the mouse muscle, adult-type AChR, the rat $\alpha1\beta1\gamma2$L $GABA_AR$, the human $\alpha1$ GlyR, the human $\alpha1\beta$ GlyR, the rat GluA1-flip AMPAR, the rat GluA1-flip/GluA2-flop AMPAR and the rat $P2X_2R$. To avoid the ambiguities associated with the slow perfusion of whole cells (and thus, for example, to make sure that the concentration of neurotransmitter in the channel-bathing solution remains as close to zero as possible during most of each interpulse interval), we used fast-perfused outside-out patches (solution-exchange time $\approx 100\ \mu s$). To minimize the time-dependent changes in the kinetics of conformational transitions that, typically, accompany patch excision (Supplemental Fig. 2 and Supplemental Table 2; see also Frosch *et al.* 1992; Lester & Jahr, 1992; Lester & Dani, 1994; Mott *et al.* 2001), the 50 Hz trains were applied within a narrow time window upon obtaining the outside-out patches, and only one such train was applied to any given patch of membrane. To ensure uniformity, all the receptors were subjected to the same stimulation protocols, the same expression system and the same saline solutions. Also, to gain a more complete understanding of the postsynaptic response to physiological trains of presynaptic action potentials, we applied several tens of neurotransmitter pulses with each train, not just pairs.

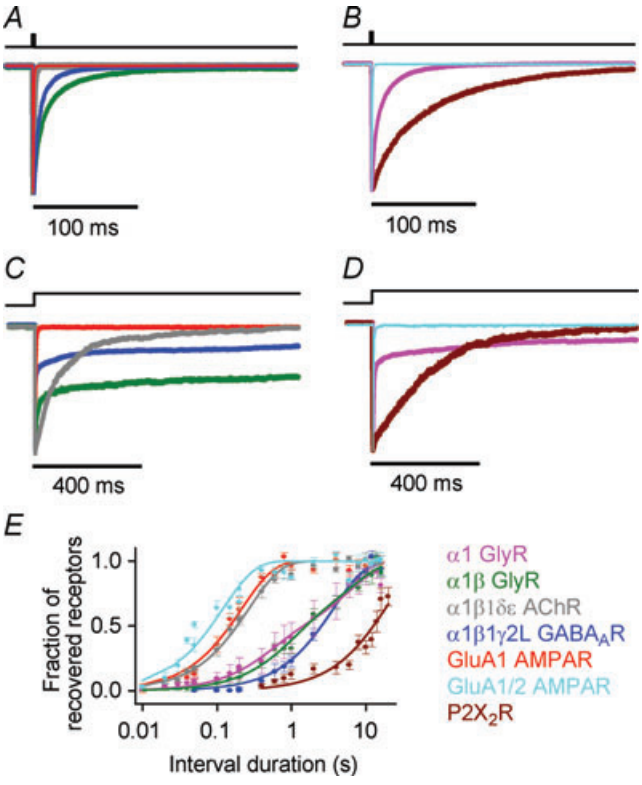

Figure 2. Kinetics of channel deactivation and desensitization
A and *B*, deactivation. Normalized current traces recorded from individual outside-out patches containing the indicated receptor channels. For clarity, the traces are displayed in two separate panels. For each receptor, consecutive responses to 1 ms pulses of saturating neurotransmitter applied as low-frequency trains were averaged. The concentration of each neurotransmitter was as indicated for Fig. 1. The estimated kinetic parameters are listed in Table 1. The colour code is the same for all panels. *C* and *D*, entry into desensitization. Normalized current traces recorded from individual outside-out patches upon stepping the concentration of neurotransmitter from zero to saturating. The estimated kinetic parameters are listed in Table 1. Although the responses recorded from individual patches exhibited high patch-to-patch variability, the traces shown in panels *A–D* are representative of the average behaviour of each receptor. *E*, recovery from desensitization. The kinetics of recovery were estimated using pairs of conditioning (1 s) and test (100 ms) pulses of saturating neurotransmitter with interpulse intervals of variable duration. Vertical error bars are standard errors calculated from the results of several independent experiments (one experiment per patch). The estimated kinetic parameters are listed in Table 1.

As is clear from Fig. 1, the peak responses of all studied receptors decline within the applied 50 Hz stimulus trains. Since the peak currents recover their full amplitude after prolonged exposure to solutions without neurotransmitter (Fig. 2), we rule out the possibility that mechanisms such as receptor internalization contribute to the observed fading of the current responses. Rather, we attribute the observed phenomenon to receptor-channel desensitization. A closer inspection of the current traces in Fig. 1 indicates that, disregarding desensitization potentially occurring during the rising phase, the depression of the peak-current amplitudes cannot be accounted for by entry into desensitization during the ~1 ms neurotransmitter pulses alone, (Fig. 3). Furthermore, the traces in Fig. 1 show that the declining peak-current amplitudes within a train of responses tend to a steady-state level consistent with the idea that the number of channels that enter the desensitized state(s) between the beginning of one pulse and the beginning of the next one eventually approaches the number of desensitized channels that recover during these intervals. Also consistent with the entry-into and recovery-from desensitization phenomenon, these steady-state values decrease as the train frequency increases (Figs 4 and 5), eventually becoming identical to the current elicited in response to the continuous application of neurotransmitter (Fig. 6).

To test the possibility that an incomplete neurotransmitter washout between consecutive pulses enhanced the observed extent of desensitization, we measured the kinetics of deactivation of individual responses within a train for trains applied at different frequencies. A poor removal of the neurotransmitter would lead to its progressive accumulation toward the end of the stimulus train, and this accumulation would be more pronounced as the train frequency increases. Such an accumulation of the neurotransmitter, in turn, would manifest as a slower decay of the current transients.

Gratifyingly, and in keeping with the time course of agonist application and washout inferred from the open-tip potential measurements (see Methods), we found that the decay kinetics are essentially the same regardless of the relative position of the measured response within a train, or of the frequency of the stimulation (tested range: 1–50 Hz). Moreover, we also increased the concentration of the different neurotransmitters by a factor of 10 from already saturating values. Again, an incomplete removal of the agonist between consecutive applications would manifest as a slower decay of the currents for the responses recorded at higher neurotransmitter concentrations. Kinetic analysis of these currents, however, failed to reveal consistent differences between the responses elicited by these two stimulation protocols. We conclude that, in our experiments, the concentration of neurotransmitter is nearly zero during the interpulse intervals.

To gain a more quantitative understanding of the extent to which desensitization occurs within and between neurotransmitter pulses, we calculated the responses to repetitive stimulation of two example NGICs that display widely different kinetics (Fig. 2 and Table 1): the $P2X_2R$ and the muscle AChR. To this end, we applied Q-matrix methods (Colquhoun & Hawkes, 1995*a*) to established kinetic models (Fig. 7*A* and *B*) of these two channels. These calculations (Fig. 8), in which the application and removal of neurotransmitter were modelled as being infinitely fast, amply confirm the notion derived from Fig. 3, namely, that desensitization upon high-frequency stimulation occurs, to a large degree, during the interpulse intervals.

Extent of receptor saturation

The fraction of postsynaptic receptors that interact with the neurotransmitter released upon arrival of a presynaptic action potential, commonly referred to as the 'extent of saturation', is not necessarily unity (Clements, 1996; Frerking & Wilson, 1996; Silver *et al.* 1996; Xu-Friedman & Regehr, 2004). As a result, and assuming that neurotransmitter molecules impinge on a random subset of receptors every time they are released, the mean frequency at which each individual postsynaptic receptor interacts with neurotransmitter may be only a fraction of the frequency of the incoming train of action potentials. Because the extent of depression decreases as the train frequency is reduced (Figs 4 and 5), one can expect that the lower the extent of saturation, the lower the degree of depression owing to desensitization.

In our experiments, the relative diameters of the patch-pipette and the perfusion-pipette openings ensure that all the channels in the patch have the opportunity to interact with neurotransmitter every time a pulse is applied. As a result, our experimental approach provides an upper-limit estimate of the extent of depression. To visualize with numerical examples how the extent of receptor saturation would affect the extent of depression, we calculated the expected responses of two NGICs to repetitive, 50 Hz stimulation (Fig. 9). These channels are the wild-type AMPAR (Fig. 7*C*) and a hypothetical muscle-AChR mutant having a gating equilibrium constant that is larger than the wild-type's by a factor of 10 (not an uncommon value for an AChR gain-of-function mutant) so as to accentuate the decline of the peak responses (Elenes *et al.* 2006, 2009).

The calculations in Fig. 9 were performed as for Fig. 8, applying Q-matrix methods (Colquhoun & Hawkes,

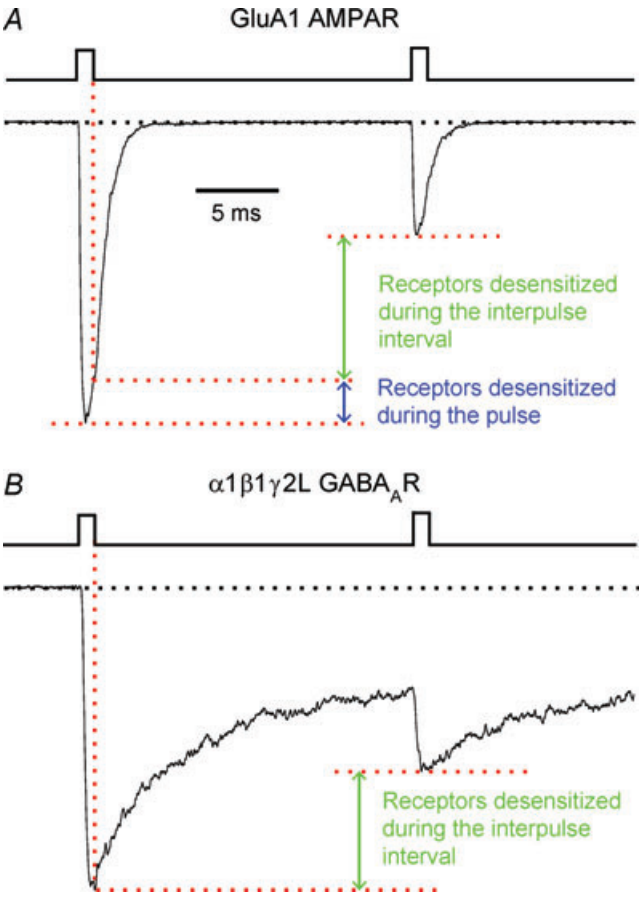

Figure 3. Desensitization during the interpulse intervals
A, response of an outside-out patch containing GluA1 AMPARs to the application of a 50 Hz train of 1 ms pulses of 10 mM Glu magnified so as to show only the first two current transients. The zero-current level is indicated with a black dotted line. Disregarding desensitization potentially occurring during the rising phase, the red dotted lines help distinguish the extent to which desensitization occurs during the 1 ms application of Glu (blue arrow) from that occurring in between applications (green arrow). Because desensitized receptors can recover during the interpulse intervals, the extent of desensitization may actually be larger than that indicated by the green arrow. *B*, response of an outside-out patch containing $\alpha1\beta1\gamma2L$ $GABA_A$Rs to the application of a 50 Hz train of 1 ms pulses of 10 mM GABA. As in *A*, only the first two current transients are shown.

1995*a*) to established kinetic models with the added feature that only a random fraction of the total population of channels was allowed to interact with the neurotransmitter (and, thus, to desensitize) every time the response to a pulse of neurotransmitter was calculated. This fractional value (which we denote, here, as p) was kept constant throughout each train and represents the extent of receptor saturation.

As shown in Fig. 9*B* and *D*, lower saturation values attenuate the extent of depression for both kinetic models but, as shown in Fig. 9*A* and *C*, the peak values of the currents calculated for lower-saturation, less-depressing synapses never exceed those from synapses with higher extents of saturation to a large degree. Clearly, at least for the two kinetic models examined here, reducing the extent of depression by decreasing receptor saturation would not convert a failing synapse into a reliable one, even when the depression could be much less pronounced.

It is worth noting here that estimates of NGIC saturation in many intact synapses are closer to unity than they are to zero (Clements *et al.* 1992; Faber *et al.* 1992; Tong & Jahr, 1994; Silver *et al.* 1996; Auger & Marty, 1997; Harrison & Jahr, 2003). Therefore, the fact that the channel responses studied here (Fig. 1, for example) were recorded under conditions of full saturation need not be a major concern.

The case of the ganglionic AChRs

Initially, we intended to include the $\alpha3\beta4$ AChR (considered to be the main contributor to the α-bungarotoxin-insensitive component of the postsynaptic ganglionic currents) in this study, and thus, to subject it to the same protocols of pulses that we applied to all other NGICs. However, we found that the rise time of the currents through this AChR is too slow for appreciable currents to develop during 1 ms ACh pulses, which prompted us to prolong the pulses to 5 ms (Fig. 10). Furthermore, we found that the peak responses decline on repetitive stimulation much more profoundly for the $\alpha3\beta4$ AChR than for any of the other channels under consideration, to the point that we could only run a single stimulation protocol per patch of membrane even at train frequencies as low as 1 Hz. Whether shorter ACh pulses (closer in duration, perhaps, to the ACh transients in intact autonomic ganglia) reduce the fraction of AChRs that desensitize by virtue of their activating fewer channels remains to be ascertained. Our attempts so far to address this question have been hampered by the profound decline of the currents, which precludes the repetitive application of pulses of different duration to the same patch of membrane.

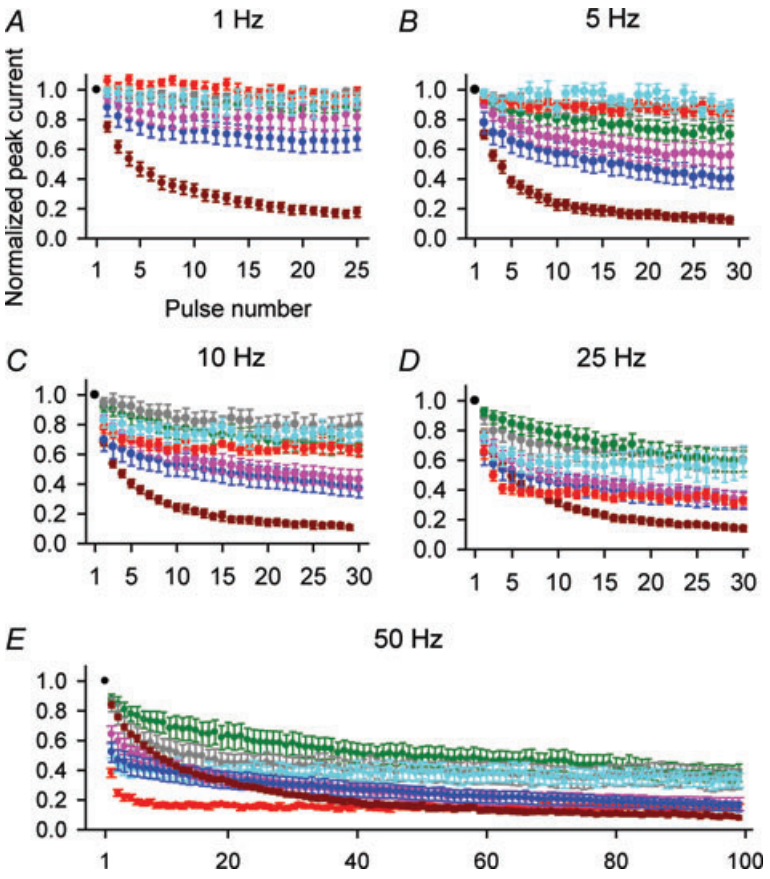

Figure 4. Frequency dependence of the rate and extent of depression
A–E, normalized peak-current responses to trains of neurotransmitter pulses delivered at different physiologically relevant frequencies. The colour code is the same as for Fig. 2. The concentration of each neurotransmitter was as indicated for Fig. 1. The number of trains averaged for each receptor–frequency combination ranged between 9 and 14. Only one train at any given frequency was applied per patch. Error bars are standard errors. The point corresponding to the first pulse in each train (black symbol) is, of course, the same for all trains. Using the steady-state peak response as a parameter, the rank order of depression upon 1 Hz stimulation is (from the lowest, most depressed steady-state response to the highest): $P2X_2R > \alpha1\beta2\gamma2L$ $GABA_AR > \alpha1$ GlyR $> \alpha1\beta$ GlyR $\approx$ GluA1 AMPAR $\approx$ GluA1/2 AMPAR $\approx \alpha1\beta1\delta\varepsilon$ AChR, whereas, upon 50 Hz stimulation, the order is: $P2X_2R >$ GluA1 AMPAR $\approx \alpha1$ GlyR $\approx \alpha1\beta2\gamma2L$ $GABA_AR >$ GluA1/2 AMPAR $\approx \alpha1\beta$ GlyR $\approx \alpha1\beta1\delta\varepsilon$ AChR. Using the peak response to the 10th pulse of a 50 Hz train as a parameter, the rank order is GluA1 AMPAR $>$ GluA1/2 AMPAR $\approx \alpha1\beta2\gamma2L$ $GABA_AR \approx \alpha1$ GlyR $\approx P2X_2R > \alpha1\beta1\delta\varepsilon$ AChR $> \alpha1\beta$ GlyR.

As a step toward elucidating whether co-assembly of the $\alpha 3$ subunit with other subunits also known to be part of ganglionic AChRs gives rise to receptors that respond more reliably to trains of ACh than does the $\alpha 3\beta 4$ combination in outside-out patches, we added cDNA encoding the $\alpha 5$ subunit (Vernallis *et al.* 1993) to the $\alpha 3$–$\beta 4$ cDNA transfection mixture. As judged from the higher single-channel conductance and shorter mean duration of the recorded bursts of single-channel openings, we conclude that the $\alpha 5$ subunit became successfully incorporated into functional AChRs. Indeed, bursts of openings of the sort recorded from cells transfected with the $\alpha 3$–$\beta 4$ cDNA mixture alone were only infrequently observed. In most patches, the incorporation of the $\alpha 5$ subunit did not affect the response to repetitive stimulation, inasmuch as the peak currents also declined irreversibly along low-frequency trains of 1 mM ACh. In a few patches, however, the currents did maintain a rather constant peak amplitude throughout the 1 Hz stimulation protocol (Fig. 10), a behaviour that resembles more closely the response of most other NGICs to trains delivered at this low frequency (Fig. 4*A*). Further characterization of the responses of $\alpha 3$-subunit-containing AChRs to stimulus trains is needed to clarify the unique functional properties of these AChRs under conditions of synaptic-like stimulation.

Discussion

In this study, we decided to investigate postsynaptic mechanisms of short-term plasticity in detail. Thus, our priority was to maximize the accuracy of the electrophysiological recordings and to eliminate variables that could lead to ambiguities in their interpretation. To accomplish this goal, we chose to use fast-perfused outside-out patches from transiently transfected cells and showed that all studied channels desensitize upon repetitive stimulation to an appreciable degree. To our

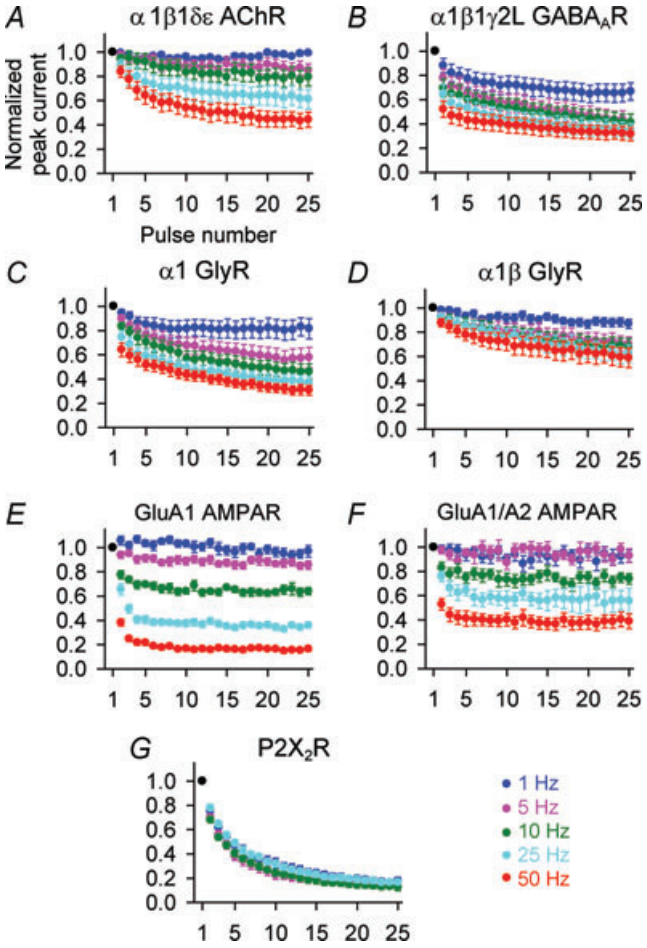

Figure 5. Frequency dependence of depression
Normalized peak responses to trains of neurotransmitter pulses. Error bars are standard errors. The point corresponding to the first pulse in each train (black symbol) is the same for all trains. The data in all seven panels were re-plotted from Fig. 4. The colour code is: 1 Hz, blue; 5 Hz, purple; 10 Hz, green; 25 Hz, cyan; and 50 Hz, red. The concentration of each neurotransmitter was as indicated for Fig. 1. The remarkably slow recovery from desensitization of the P2X$_2$R (Fig. 2*E* and Table 1) explains in part this receptor's pronounced depression even in response to low-frequency repetitive stimulation. For clarity, the plot corresponding to the response of the P2X$_2$R to 50 Hz trains is omitted.

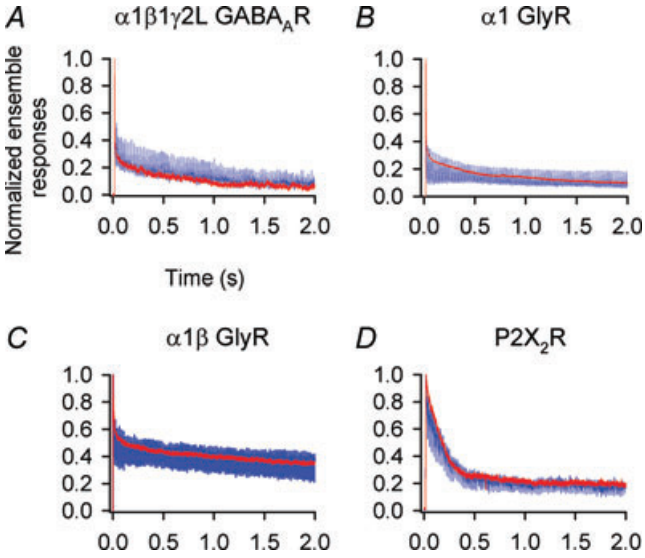

Figure 6. Responses to high-frequency repetitive *versus* continuous application of neurotransmitter
Normalized current traces recorded from individual outside-out patches upon the repetitive (50 Hz trains of 1 ms pulses; blue) or continuous (red) application of saturating neurotransmitter. For each receptor, both responses were recorded from the same patch. *A*, $\alpha 1\beta 2\gamma 2$L GABA$_A$R; [GABA] = 10 mM. *B*, $\alpha 1$ GlyR; [Gly] = 10 mM. *C*, $\alpha 1\beta$ GlyR; [Gly] = 10 mM. *D*, P2X$_2$R; [ATP] = 0.85 mM. For these four NGICs, the responses to 50 Hz stimulation superimpose very well with the responses to long pulses of neurotransmitter. For the $\alpha 1\beta 1\delta\varepsilon$ AChR and the AMPARs, even higher frequencies would be needed for the two types of response to converge.

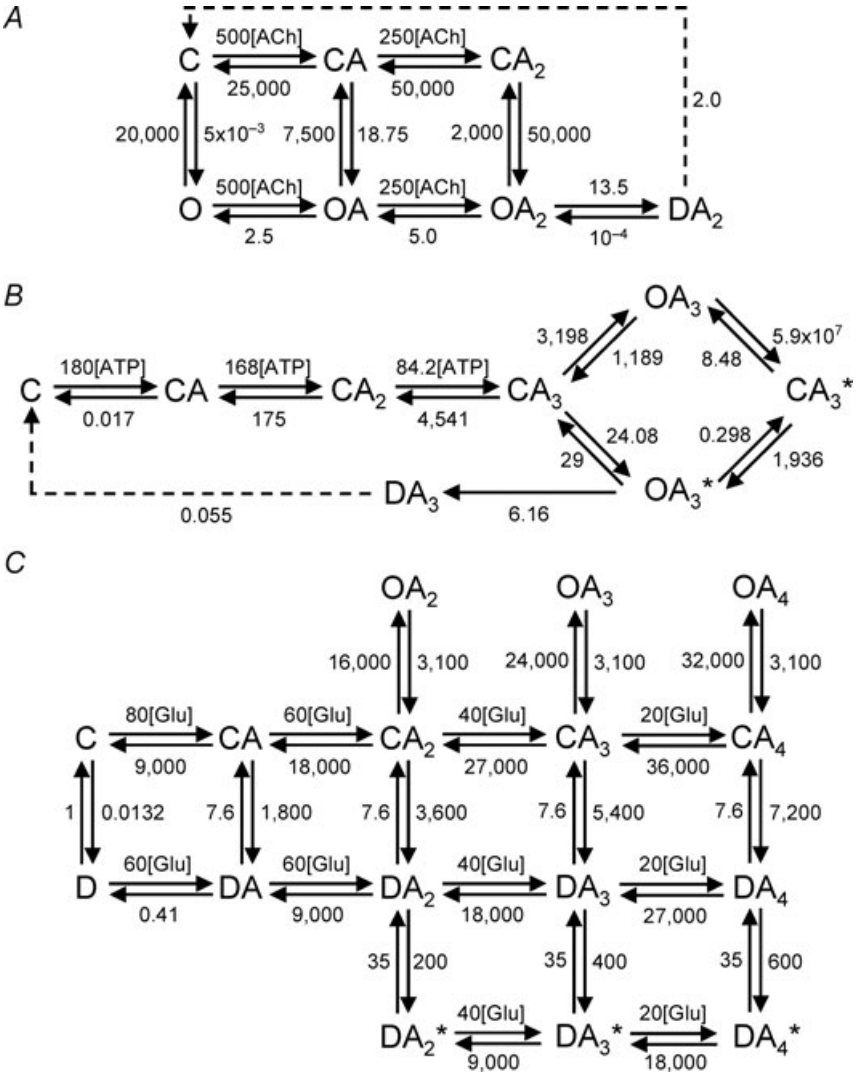

Figure 7. Kinetic models used for Q-matrix calculations
'A' denotes a molecule of bound neurotransmitter, whereas 'C', 'O' and 'D' denote the closed, open and desensitized conformations of the channel, respectively. Neurotransmitter-association rate constants are given in units of $\mu M^{-1}\ s^{-1}$; all other rate constants are given in units of s^{-1}. *A*, a model of the adult-muscle $\alpha 1\beta 1\delta\varepsilon$ AChR. The values of the rate constants of ACh association to and dissociation from the open-channel conformation are poorly defined, and our numbers are only tentative; the same is the case for the rate constants of interconversion between closed and open states of unliganded and mono-liganded $\alpha 1\beta 1\delta\varepsilon$ AChRs. However, changing any of these values by an order of magnitude in either direction does not appreciably affect the calculated responses to repetitive stimulation. The time course of deactivation calculated with this model was best fitted with a time constant of 0.99 ms, whereas the experimentally recorded time course was best fitted with a time constant of 1.11 ms (Table 1). The calculated time course of entry into desensitization was best fitted with a single-component exponential function with a half-time of 53.8 ms, whereas the experimentally recorded double-exponential time course has a half-time of 51.2 ms (Table 1). *B*, a model of the $P2X_2R$. This model (without the desensitized state, DA_3) was originally proposed by Ding & Sachs (1999), and modifications to the originally proposed set of rate constant values were suggested by Moffatt & Hume (2007). Q-matrix calculations using the latter set of values matched our experimental observations quite closely, but an even better agreement with the responses to repetitive stimulation was obtained upon increasing the three ATP-association rate constants by a factor of 10. A desensitized state was added to the model with rate constants of entry and recovery calculated from our own experimental results. The asterisks in CA_3* and OA_3* indicate alternative conformations of the closed and the open triply liganded states. We note that the unusually fast rate constant from OA_3 to CA_3* could be reduced by a factor of 10^4 without qualitatively affecting the calculated responses to repetitive stimulation. Also, the cycle of triply liganded states does not obey the principle of detailed balance, a feature we can neither confirm nor disprove with our experimental data. Although other kinetic models have been proposed to provide a better description of this channel's behaviour (Moffatt & Hume, 2007), the model in *B* seemed adequate for our purposes. The time course of deactivation calculated with this model was best fitted with a single-component exponential function

knowledge, this is the first time the current responses of members of all three superfamilies of NGICs to a synaptic-like application of neurotransmitter are recorded under identical experimental conditions, thereby allowing the direct comparison of their behaviours. Furthermore, for some of these channels, this may be the first time that their response to long trains of high-frequency stimulation was recorded at all.

Of course, it could be argued that the relevant auxiliary proteins and posttranslational modifications that occur in native postsynaptic membranes may not be present in a heterologous expression system such as that we employed here. It is precisely for this reason that our results should be regarded as a starting point that defines the behaviour of these channels in a sort of 'basal' or 'minimal' state. Future work will have to address the functional impact of these ancillary proteins and chemical modifications, although these remain (with only a few exceptions; e.g., Cho *et al.* 2007; Tomita, 2010) largely unknown for most NGICs. It could also be argued that 1 ms pulses are much longer than typical exposure times to neurotransmitter in the context of a synapse, but our finding that desensitization occurs, to a large degree, between pulses (as opposed to within pulses) should lessen this concern. In summary, to the extent that our experimental approach recapitulates the most important aspects of NGIC function at the postsynaptic membrane, our results clearly indicate that channel desensitization has the potential to contribute to short-term depression much like well-studied presynaptic mechanisms, such as vesicle depletion, can. By no means, however, do we mean to imply that desensitization will necessarily lead to synaptic transmission failure. Whether the depression of the peak-current amplitudes is profound enough to prevent the postsynaptic cell from generating an action potential ultimately depends on the properties of each particular synapse. For example, in normal human subjects, it has been shown that synaptic transmission

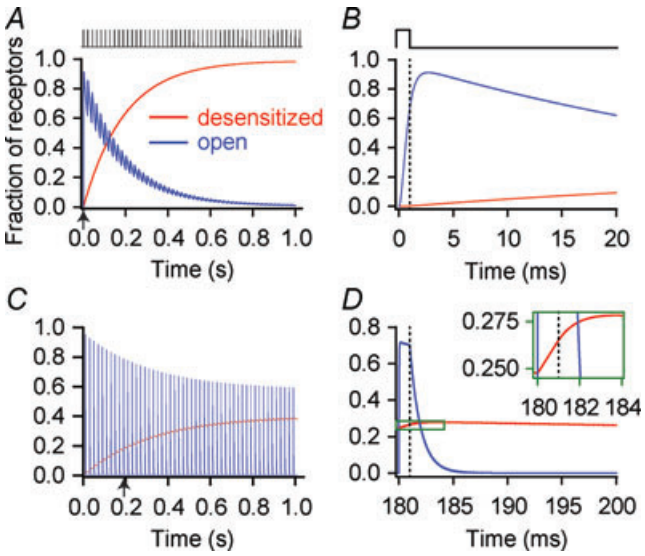

Figure 8. Open- *versus* desensitized-state occupancies
Calculated time courses corresponding to the $P2X_2R$ and the $\alpha1\beta1\delta\varepsilon$ AChR in response to 50 Hz trains of 1 ms pulses of saturating neurotransmitter. The calculations were done by applying Q-matrix methods (Colquhoun & Hawkes, 1995*a*) to established kinetic models of these two channels (Fig. 7*A* and *B*). The occupancy of the open state (blue lines) includes the occupancies in all open states, regardless of their degree of ligation. *A* and *B*, $P2X_2R$; [ATP] = 0.85 mM. In *B*, the time course during the first 20 ms (corresponding to the first pulse of neurotransmitter and the first interpulse interval; see vertical arrow in *A*) is shown at an expanded time scale. The vertical dashed line denotes the end of the 1 ms pulse. The colour code is the same for all panels. *C* and *D*, $\alpha1\beta1\delta\varepsilon$ AChR; [ACh] = 1 mM. In *D*, the time course during the 20 ms interval corresponding to the tenth pulse of neurotransmitter and its corresponding interpulse interval (see vertical arrow in *C*) is shown at an expanded time scale. The vertical dashed line denotes the end of the 1 ms pulse. The inset is a further magnified view of the data in the green rectangle. Panels *A* and *C* show how these channels accumulate in the desensitized state along trains of stimuli. Panels *B* and *D* show that a large fraction of this desensitization takes place during the interpulse intervals.

with a half-time of 30.2 ms, whereas the experimentally recorded double-exponential time course has a half-time of 32.2 ms (Table 1). The calculated time course of desensitization was best fitted with a single exponential function with a half-time of 119 ms, whereas the experimentally recorded double-exponential time course has a half-time of 114 ms (Table 1). For both the muscle AChR and the $P2X_2R$, recovery from desensitization during the interpulse intervals was modelled as a single-step transition (dashed arrow) between the fully liganded desensitized state and the unliganded closed state even when several individual steps of neurotransmitter dissociation and conformational change must clearly occur. This simplification is justified, however, because the time course of recovery from desensitization upon neurotransmitter removal was well approximated by a single-component exponential function for these two channels (Fig. 2*E* and Table 1) and because the values of the rate constants corresponding to the individual steps between states DA_n and C are not known. Another simplification is the inclusion of a single fully liganded desensitized state even though these channels are very likely to adopt multiple desensitized conformations (e.g. Feltz & Trautmann, 1982; Paradiso & Brehm 1998; Elenes & Auerbach, 2002). None of these simplifications, however, affect the conclusions drawn here. *C*, a model of the GluA1 receptor taken from the work of Robert & Howe (2003). The time course of deactivation calculated with this model was best fitted with a time constant of 0.92 ms, whereas the experimentally recorded time course was best fitted with a time constant of 0.57 ms (Table 1). The calculated time course of desensitization was best fitted with a time constant of 1.91 ms, whereas the experimentally recorded time course was best fitted with a time constant of 2.65 ms (Table 1).

at the neuromuscular junction rarely fails even during extreme exertion (Bigland-Ritchie *et al.* 1982) and, in some GABAergic cerebellar synapses, a number of adaptations seem to have evolved that keep $GABA_AR$ desensitization from compromising the reliability of synaptic transmission (Pugh & Raman, 2005). On the other hand, at least in some glutamatergic synapses, AMPAR desensitization upon high-frequency stimulation has been proposed to contribute to curtailing the postsynaptic train of responses, and thus would have behavioural consequences (Trussell, 1999; Brenowitz & Trussell, 2001; Wall *et al.* 2002; Chanda & Xu-Friedman, 2010). At fast chemical synapses mediated by other neurotransmitters, the relationship between channel desensitization and synaptic transmission failure has been investigated in less detail.

Another conclusion that follows from our results is that an incomplete clearance of neurotransmitter from the synaptic cleft between vesicle-fusion events need not be invoked to account for NGIC desensitization upon repetitive stimulation. Certainly, our data suggest that, for all tested NGICs, entry into desensitization contributes to the time course of deactivation (that is, the decay of the current in the complete absence of agonist). Evidently, if neurotransmitter removal were slower or less complete than that under our experimental conditions (as is likely to be the case, at least, for some synapses) channel desensitization would be even more pronounced.

Of all eight receptor channels studied here, the $\alpha 3$ subunit-containing AChRs were the only ones whose responsiveness to neurotransmitter was lost in a seemingly irreversible manner upon repeated application of ligand. Such a strongly depressing response to low-frequency repetitive stimulation (1 Hz in Fig. 10) is surprising for a receptor thought to mediate fast synaptic transmission at autonomic ganglia, but our finding is not entirely unexpected. Previous studies on the behaviour of human (Nelson & Lindstrom, 1999) and rat (Sivilotti

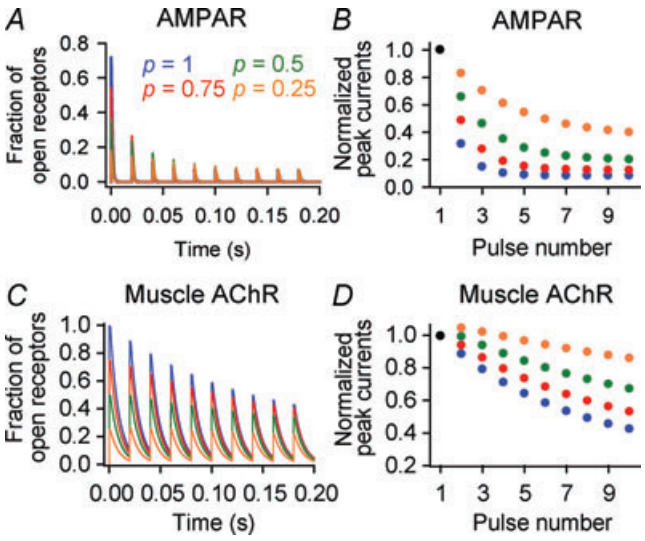

Figure 9. Effect of extent of receptor saturation on depression
A, calculated macroscopic currents through the wild-type GluA1 AMPAR in response to 50 Hz trains of 1 ms pulses of (saturating) 10 mM Glu. The kinetic model in Fig. 7*C* was used. *p* represents the extent of saturation. The colour code is the same for all panels. *B*, normalized peak responses calculated from the data in *A*. The point corresponding to the first pulse in each train (black symbol) is the same for all trains. *C*, calculated macroscopic currents through a hypothetical gain-of-function mutant of the $\alpha 1\beta 1\delta\varepsilon$ AChR in response to 50 Hz repetitive stimulation, as in *A*. The (saturating) concentration of ACh used for this calculation was 1 mM. The only difference with the kinetic model of the wild-type muscle AChR in Fig. 7*A* is that the diliganded gating equilibrium constant was increased by a factor of 10 (by slowing down the corresponding closing rate constant while keeping the opening rate constant unchanged) so as to increase the extent of depression (Elenes *et al.* 2006, 2009). To maintain detailed balance, the gating equilibrium constants of the un- and monoliganded receptors were also increased by a factor of 10 by, in this case, speeding up the corresponding opening rate constants. It is important to realize, however, that the precise way in which these changes in equilibrium constants are brought about by changes in the underlying forward and backward rate constants has a negligible effect on the calculated currents and is, hence, irrelevant to our conclusions. *D*, normalized peak responses calculated from the data in *C*. At $p = 0.25$, the calculated peak responses display some facilitation (see the larger-than-unity responses to the second and third pulses of ACh) resulting from the summation of consecutive current responses. This phenomenon is favoured by the combination of a low extent of saturation and the very slow deactivation time course of this hypothetical mutant AChR.

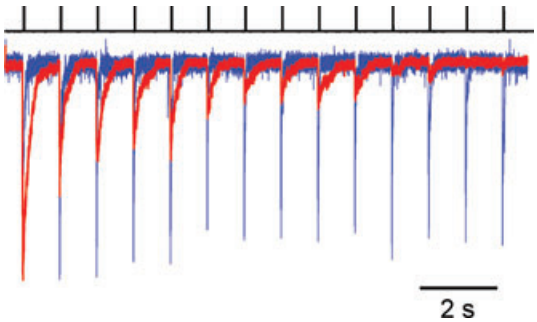

Figure 10. The $\alpha 3\beta 4$ AChR and the effect of the $\alpha 5$ subunit
Normalized current traces recorded from individual outside-out patches excised from cells transfected with human $\alpha 3$ and $\beta 4$ (red trace) or human $\alpha 3$, $\alpha 5$ and $\beta 4$ (blue trace) AChR-subunit cDNAs. cDNA encoding human RIC-3, a chaperone (Lansdell *et al.* 2005), was also included in all transfection mixtures. Currents were elicited by the application of a 1 Hz train of 5 ms pulses of 1 mM ACh. The stimulus train is indicated above the current traces. The trace shown in red is representative of all the recordings (10 out of 10) obtained from cells transfected with a $\alpha 3$:$\beta 4$:RIC-3 1:1:1 cDNA mixture. Further applications of 1 mM ACh pulses to patches of membrane displaying this extreme decline of the peak currents elicited no response even after prolonged, several-minute-long incubations in the absence of ACh. The trace shown in blue, however, is representative of only a minor fraction of the recordings (3 out of 15) obtained from cells transfected with a $\alpha 3$:$\alpha 5$:$\beta 4$:RIC-3 1:1:1:1 cDNA mixture; the rest of these recordings were indistinguishable from those obtained with the $\alpha 3$-$\beta 4$-RIC-3 mixture alone.

et al. 1997) ganglionic AChRs in outside-out patches excised from native neurons reported the quick loss of single-channel activity in the continuous presence of low concentrations of agonist. More recently, work by Cooper and coworkers on native neurons from mouse and rat superior cervical ganglion (Campanucci *et al.* 2008, 2010) indicated that the irreversible decay of the peak currents is the result of the oxidation of the M1–M2-loop cysteine of the α3 AChR subunit (that is, the residue preceding the well-conserved glycine–glutamate–lysine motif of the AChR's charge-selectivity filter). Whether the fading of the peak-current responses we observed for human ganglionic AChRs in outside-out patches pulled from HEK-293 cells reflects this same redox phenomenon and, if this were the case, whether oxidation of the same intracellular cysteines is the culprit, remains to be determined.

Although we used specific kinetic schemes for some of the calculations in this paper, it should be noted that several of the features of these models were chosen arbitrarily and that the experiments described here were not designed to cast light on these elusive mechanistic aspects. Most notably, the extent to which the desensitized state(s) of the various NGICs is reached from the closed- *versus* the open-channel conformation (clearly, one of the most vexing and long-standing questions; e.g. Lin & Stevens, 1994; Colquhoun & Hawkes, 1995*b*) remains essentially unresolved. Despite this uncertainty, we modelled entry into desensitization of the muscle AChR (Fig. 7*A*) and the $P2X_2R$ (Fig. 7*B*) as proceeding exclusively from the open-channel conformation, whereas desensitization of the GluA1 AMPAR was modelled as proceeding only from the closed-channel conformation (Fig. 7*C*). It is important to emphasize, though, that this gap in our mechanistic understanding of the desensitization phenomenon has no bearing whatsoever on the main conclusion of this paper: namely, that all tested NGICs desensitize appreciably upon repeated stimulation at physiologically-relevant frequencies. Other simplifications used for the kinetic modelling of these receptor channels, and their irrelevance to our conclusions, are discussed in the legend to Fig. 7.

Finally, we also conclude that meaningful attempts to describe the behaviour of NGICs and their mutants in terms of rate constants of kinetic schemes need to include the (often ignored) desensitization phenomenon. Indeed, the notion that desensitization contributes to shape the deactivation time course indicates that even single-channel events recorded at very low concentrations of neurotransmitter could be misinterpreted in terms of mechanisms if desensitization were disregarded see Elenes *et al.* (2006, 2009) for the particular case of the wild-type and gain-of-function mutants of the muscle AChR).

References

Abbott LF & Regehr WG (2004). Synaptic computation. *Nature* **431**, 796–803.

Auger C & Marty A (1997). Heterogeneity of functional synaptic parameters among single release sites. *Neuron* **19**, 139–150.

Bigland-Ritchie B, Kukulka CG, Lippold OCJ & Woods JJ (1982). The absence of neuromuscular transmission failure in sustained maximal voluntary contractions. *J Physiol* **330**, 265–278.

Brenowitz S & Trussell LO (2001). Minimizing synaptic depression by control of release probability. *J Neurosci* **21**, 1857–1867.

Burzomato V, Beato M, Groot-Kormelink PJ, Colquhoun D & Sivilotti LG (2004). Single-channel behavior of heteromeric $\alpha1\beta$ glycine receptors: an attempt to detect a conformational change before the channel opens. *J Neurosci* **24**, 10924–10940.

Campanucci VA, Krishnaswamy A & Cooper E (2008). Mitochondrial reactive oxygen species inactivate neuronal nicotinic acetylcholine receptors and induce long-term depression of fast nicotinic synaptic transmission. *J Neurosci* **28**, 1733–1744.

Campanucci VA, Krishnaswamy A & Cooper E (2010). Diabetes depresses synaptic transmission in sympathetic ganglia by inactivating nAChRs through a conserved intracellular cysteine residue. *Neuron* **66**, 827–834.

Chanda S & Xu-Friedman MA (2010). A low-affinity antagonist reveals saturation and desensitization in mature synapses in the auditory brainstem. *J Neurophysiol* **103**, 1915–1926.

Chen C, Blitz DM & Regehr WG (2002). Contributions of receptor desensitization and saturation to plasticity at the retinogeniculate synapse. *Neuron* **33**, 779–788.

Chen G, Harata NC & Tsien RW (2004). Paired-pulse depression of unitary quantal amplitude at single hippocampal synapses. *Proc Natl Acad Sci U S A* **101**, 1063–1068.

Cho CH, St-Gelais F, Zhang W, Tomita S & Howe JR (2007). Two families of TARP isoforms that have distinct effects on the kinetic properties of AMPA receptors and synaptic currents. *Neuron* **55**, 890–904.

Clements JD (1996). Transmitter timecourse in the synaptic cleft: its role in central synaptic function. *Trends Neurosci* **19**, 163–171.

Clements JD, Lester RA, Tong G, Jahr CE & Westbrook GL (1992). The time course of glutamate in the synaptic cleft. *Science* **258**, 1498–1501.

Colquhoun D & Hawkes AG (1995*a*). A Q-matrix cookbook. In *Single-Channel Recording*, ed. Sakmann B & Neher E, pp. 589–633, Plenum Press, New York.

Colquhoun D & Hawkes AG (1995*b*). Desensitization of *N*-methyl-D-aspartate receptors: A problem of interpretation. *Proc Natl Acad Sci U S A* **92**, 10327–10329.

Ding S & Sachs F (1999). Single channel properties of P2X2 purinoceptors. *J Gen Physiol* **113**, 695–719.

Dudel J, Schramm M, Franke C, Ratner E & Parnas H (1999). Block of quantal end-plate currents of mouse muscle by physostigmine and procaine. *J Neurophysiol* **81**, 2386–2397.

Elenes S & Auerbach A (2002). Desensitization of diliganded mouse muscle nicotinic acetylcholine receptor channels. *J Physiol* **541**, 367–383.

Elenes S, Ni Y, Cymes GD & Grosman C (2006). Desensitization contributes to the synaptic response of gain-of-function mutants of the muscle nicotinic receptor. *J Gen Physiol* **128**, 615–627.

Elenes S, Decker M, Cymes GD & Grosman C (2009). Decremental response to high-frequency trains of acetylcholine pulses but unaltered fractional Ca^{2+} currents in a panel of "slow-channel syndrome" nicotinic receptor mutants. *J Gen Physiol* **133**, 151–169.

Faber DS, Young WS, Legendre P & Korn H (1992). Intrinsic quantal variability due to stochastic properties of receptor-transmitter interactions. *Science* **258**, 1494–1498.

Feltz A & Trautmann A (1982). Desensitization at the frog neuromuscular junction: a biphasic process. *J Physiol* **322**, 257–272.

Fortune E & Rose GJ (2001). Short-term synaptic plasticity as a temporal filter. *Trends Neurosci* **24**, 381–385.

Franke C, Parnas H, Hovav G & Dudel J (1993). A molecular scheme for the reaction between acetylcholine and nicotinic channels. *Biophys J* **64**, 339–356.

Frerking M & Wilson M (1996). Saturation of postsynaptic receptors at central synapses? *Curr Opin Neurobiol* **6**, 395–403.

Frosch MP, Lipton SA & Dichter MA (1992). Desensitization of GABA-activated currents and channels in cultured cortical neurons. *J Neurosci* **12**, 3042–3053.

Gonzalez-Gutierrez G & Grosman C (2010). Bridging the gap between structural models of nicotinic receptor superfamily ion channels and their corresponding functional states. *J Mol Biol* **403**, 693–705.

Grande LA & Spain WJ (2005). Synaptic depression as a timing device. *Physiology (Bethesda)* **20**, 201–210.

Harrison J & Jahr CE (2003). Receptor occupancy limits synaptic depression at climbing fiber synapses. *J Neurosci* **23**, 377–383.

Hennig R & Lømo T (1985). Firing patterns of motor units in normal rats. *Nature* **314**, 164–166.

Jonas P (1995). Fast application of agonists to isolated membrane patches. In *Single-Channel Recording*, ed. Sakmann B & Neher E, pp. 231–243, Plenum Press, New York.

Jones MV & Westbrook GL (1995). Desensitized states prolong $GABA_A$ channel responses to brief agonist pulses. *Neuron* **15**, 181–191.

Jones MV & Westbrook GL (1996). The impact of receptor desensitization on fast synaptic transmission. *Trends Neurosci* **19**, 96–101.

Kamboj SK, Swanson GT & Cull-Candy SG (1995). Intracellular spermine confers rectification on rat calcium-permeable AMPA and kainate receptors. *J Physiol* **486**, 297–303.

Katz B & Thesleff S (1957). A study of the desensitization produced by acetylcholine at the motor end-plate. *J Physiol* **138**, 63–80.

Koike-Tani M, Kanda T, Saitoh N, Yamashita T & Takahashi T (2008). Involvement of AMPA receptor desensitization in short-term synaptic depression at the calyx of Held in developing rats. *J Physiol* **586**, 2263–2275.

Lansdell SJ, Gee VJ, Harkness PC, Doward AI, Baker ER, Gibb AJ & Millar NS (2005). RIC-3 enhances functional expression of multiple nicotinic acetylcholine receptor subtypes in mammalian cells. *Mol Pharmacol* **68**, 1431–1438.

Lester RA & Jahr CE (1992). NMDA channel behavior depends on agonist affinity. *J Neurosci* **12**, 635–643.

Lester RA & Dani JA (1994). Time-dependent changes in central nicotinic acetylcholine channel kinetics in excised patches. *Neuropharmacol* **33**, 27–34.

Lin F & Stevens CF (1994). Both open and closed NMDA receptor channels desensitize. *J Neurosci* **14**, 2153–2160.

Liu Y & Dilger JP (1992). Desensitization of acetylcholine receptors in BC3H-1 cells. *Pflugers Arch* **420**, 479–485.

Magleby KL & Pallotta BS (1981). A study of desensitization of acetylcholine receptors using nerve-released transmitter in the frog. *J Physiol* **316**, 225–250.

Magleby KL & Stevens CF (1972). A quantitative description of end-plate currents. *J Physiol* **223**, 173–197.

Moffatt L & Hume RI (2007). Responses of rat $P2X_2$ receptors to ultrashort pulses of ATP provide insights into ATP binding and channel gating. *J Gen Physiol* **130**, 183–201.

Mott DD, Erreger K, Banke TG & Traynelis SF (2001). Open probability of homomeric murine 5-HT3A serotonin receptors depends on subunit occupancy. *J Physiol* **535**, 427–443.

Nelson ME & Lindstrom J (1999). Single channel properties of human $\alpha 3$ AChRs: impact of $\beta 2$, $\beta 4$ and $\alpha 5$ subunits. *J Physiol* **516**, 657–678.

Otis T, Zhang S & Trussell LO (1996). Direct measurement of AMPA receptor desensitization induced by glutamatergic synaptic transmission. *J Neurosci* **16**, 7496–7504.

Paradiso K & Brehm P (1998). Long-term desensitization of nicotinic acetylcholine receptors is regulated via protein kinase A-mediated phosphorylation. *J Neurosci* **18**, 9227–9237.

Partin KM, Patneau DK, Winters CA, Mayer ML & Buonanno A (1993). Selective modulation of desensitization at AMPA versus kainate receptors by cyclothiazide and concanavalin A. *Neuron* **11**, 1069–1082.

Pugh JR & Raman IM (2005). $GABA_A$ receptor kinetics in the cerebellar nuclei: evidence for detection of transmitter from distant release sites. *Biophys J* **88**, 1740–1754.

Qin, F (2004). Restoration of single-channel currents using the segmental k-means method based on Hidden Markov modeling. *Biophys J* **86**, 1488–1501.

Raman IM & Trussell LO (1995). The mechanism of α-amino-3-hydroxy-5-methyl-4-isoxazolepropionate receptor desensitization after removal of glutamate. *Biophys J* **68**, 137–146.

Robert A & Howe JR (2003). How AMPA receptor desensitization depends on receptor occupancy. *J Neurosci* **23**, 847–858.

Saviane C & Silver RA (2006). Fast vesicle reloading and a large pool sustain high bandwidth transmission at a central synapse. *Nature* **439**, 983–987.

Silver RA, Cull-Candy SG & Takahashi T (1996). Non-NMDA glutamate receptor occupancy and open probability at a rat cerebellar synapse with single and multiple release sites. *J Physiol* **494**, 231–250.

Sivilotti LG, McNeil DK, Lewis TM, Nassar MA, Schoepfer R & Colquhoun D (1997). Recombinant nicotinic receptors, expressed in *Xenopus* oocytes, do not resemble native rat sympathetic ganglion receptors in single-channel behaviour. *J Physiol* **500**, 123–138.

Stevens CF (2003). The importance of depression. *Nature* **421**, 29–30.

Swanson GT, Kamboj SK & Cull-Candy SG (1997). Single-channel properties of recombinant AMPA receptors depend on RNA editing, splice variation, and subunit composition. *J Neurosci* **17**, 58–69.

Tomita S (2010). Regulation of ionotropic glutamate receptors by their auxiliary subunits. *Physiology (Bethesda)* **25**, 41–49.

Tong G & Jahr CE (1994). Multivesicular release from excitatory synapses of cultured hippocampal neurons. *Neuron* **12**, 51–59.

Trussell LO (1999). Synaptic mechanisms for coding timing in auditory neurons. *Annu Rev Physiol* **61**, 477–496.

Vernallis AB, Conroy WG & Berg DK (1993). Neurons assemble acetylcholine receptors with as many as three kinds of subunits while maintaining subunit segregation among receptor subtypes. *Neuron* **10**, 451–464.

Wall MJ, Robert A, Howe JR & Usowicz MM (2002). The speeding of EPSC kinetics during maturation of a central synapse. *Eur J Neurosci* **15**, 785–797.

Wong AYC, Graham BO, Billups B & Forsythe ID (2003). Distinguishing between presynaptic and postsynaptic mechanisms of short-term depression during action potential trains. *J Neurosci* **23**, 4868–4877.

Xu-Friedman MA & Regehr WG (2004). Structural contributions to short-term plasticity. *Physiol Rev* **84**, 69–85.

Yamada KA & Tang CM (1993). Benzothiadiazides inhibit rapid glutamate receptor desensitization and enhance glutamatergic synaptic currents. *J Neurosci* **13**, 3904–3915.

Zucker RS & Regehr WG (2002). Short-term synaptic plasticity. *Annu Rev Physiol* **64**, 355–405.

Author contributions

All authors contributed to the conception and design of the experiments. D.P. and C.G. contributed to the collection, analysis and interpretation of data, and the drafting of the article as well as revising it critically for important intellectual content. All authors approved the final version for publication. The experiments were performed in the laboratory of C.G. at the University of Illinois at Urbana-Champaign, IL, USA.

Acknowledgements

We thank S. Elenes (Universidad de Colima, Colima, Mexico) for critical advice on fast-perfusion experiments, A. Penn (MRC Laboratory of Molecular Biology, Cambridge, UK) for suggestions regarding the expression of AMPARs, and G. Papke, M. Maybaum and J. Pizarek for technical assistance. This work was supported by National Institutes of Health (USA) grants NS042169 to C.G. and T32GM008276 to D.P.